

Author's Accepted Manuscript

An investigation of the limits of grain refinement after processing by a combination of severe plastic deformation techniques: a comparison of Al and Mg alloys

Shima Sabbaghianrad, Seyed Alireza Torbati-Sarraf, Terence G. Langdon



PII: S0921-5093(17)31550-2
DOI: <https://doi.org/10.1016/j.msea.2017.11.090>
Reference: MSA35805

To appear in: *Materials Science & Engineering A*

Received date: 12 August 2017
Revised date: 20 November 2017
Accepted date: 21 November 2017

Cite this article as: Shima Sabbaghianrad, Seyed Alireza Torbati-Sarraf and Terence G. Langdon, An investigation of the limits of grain refinement after processing by a combination of severe plastic deformation techniques: a comparison of Al and Mg alloys, *Materials Science & Engineering A*, <https://doi.org/10.1016/j.msea.2017.11.090>

This is a PDF file of an unedited manuscript that has been accepted for publication. As a service to our customers we are providing this early version of the manuscript. The manuscript will undergo copyediting, typesetting, and review of the resulting galley proof before it is published in its final citable form. Please note that during the production process errors may be discovered which could affect the content, and all legal disclaimers that apply to the journal pertain.

An investigation of the limits of grain refinement after processing by a
combination of severe plastic deformation techniques: a comparison of Al and Mg
alloys

Shima Sabbaghianrad^{1*}, Seyed Alireza Torbati-Sarraf¹, Terence G. Langdon^{1,2}

¹Departments of Aerospace & Mechanical Engineering and Materials Science University of
Southern California, Los Angeles, CA 90089-1453, U.S.A.

²Materials Research Group, Faculty of Engineering and the Environment University of
Southampton, Southampton SO17 1BJ, U.K.

*Corresponding author: Shima Sabbaghianrad, e-mail: ssabbagh@usc.edu

Abstract

An Al-7075 aluminum alloy and a ZK60 magnesium alloy were processed by a combination of equal-channel angular pressing (ECAP) for 4 passes and high-pressure torsion (HPT) through total numbers of up to 20 turns. Processing by ECAP and HPT were performed at 473 K and room temperature, respectively. Mechanical testing showed an increase in the hardness value of the Al-7075 alloy after a combination of ECAP and HPT whereas in the ZK60 alloy the hardness was reduced. Microstructural images of the Al-7075 alloy revealed very significant grain refinement after a combination of ECAP + HPT compared to the individual processing techniques. By contrast, and consistent with the hardness measurements, the average grain size of the ZK60 alloy was larger after processing by the two-step SPD technique. These results are examined and an explanation is presented based on the available microstructural evidence.

Keywords: Aluminum, equal-channel angular pressing, hardness, high-pressure torsion, magnesium, microstructure.

1. Introduction

Severe plastic deformation (SPD) techniques are well-known for refining the microstructure of metallic materials to the submicrometer or nanometer ranges with large fractions of high-angle grain boundaries [1-3]. Among the numerous SPD techniques now available, equal-channel angular pressing (ECAP) [4] and high-pressure torsion (HPT) [5] are the most common. Processing by ECAP leads to ultrafine-grained (UFG) structures in larger samples and the process is relatively simple. This process has been applied to various metallic materials leading to significant grain refinement and improvements in their mechanical properties [6-10]. The HPT process is more complex, it produces smaller samples generally in the form of thin disks but it also leads, by comparison with ECAP, to a more refined grain structure [11,12] and a higher fraction of high-angle boundaries [13]. Processing by HPT has been applied to numerous alloys and metal matrix composites [14-18] and it leads to improvements in both the tensile strength and the elongations to failure.

According to the Hall-Petch relationship, the yield stress, σ_y of a material is inversely proportional to the square root of the grain size, d , as shown by the relationship [19,20]

$$\sigma_y = \sigma_0 + k_y d^{\frac{1}{2}} \quad (1)$$

where σ_0 is the lattice friction stress and k_y is a yielding constant. This relationship shows that the strength of the material increases through a reduction in the grain size. Accordingly, several studies have been aimed at further refining the grain size in order to achieve high strength using combinations of SPD techniques including accumulative roll bonding (ARB) + friction stir processing [21], ECAP + HPT [22-29], ECAP + cold rolling (CR) [30] and ECAP + CR + HPT [30].

Several studies have also been conducted to determine or calculate the limit of grain refinement after processing by SPD techniques. Specifically, calculations were performed in which the minimum grain size was modeled after processing by ball-milling [31], ECAP [32] or HPT [33] and these minimum grain sizes were related to physical parameters including the activation energy and the stacking fault energy. Although these studies made no attempt to address the problem of combining SPD techniques, a recent review concluded that the minimum grain size achieved in single phase alloys was not dependent either upon the initial microstructure or upon any prior processing performed on the material [34].

Generally, an examination of published data shows that experimental results on the minimum grain sizes obtained from combining SPD processes are conflicting. For example, it was reported that the processing of pure Ti by a combination of ECAP + HPT led to additional grain refinement and increased microhardness and strength [22] whereas in a study on niobium it was concluded that the initial state makes no contribution to the final microstructure since similar grain sizes were obtained after processing both by HPT and by a combination of ECAP + HPT [26].

The present experiments were conducted specifically to address this dichotomy. Earlier investigations have established the microstructural characteristics and levels of grain refinement that may be achieved after processing of an Al-7075 aluminum alloy and a ZK60 magnesium alloy by single-step SPD processing using either ECAP [29,35] or HPT [36-38]. The present investigation was therefore designed to build upon these earlier results and to take the same two materials and make a direct comparison between the levels of grain refinement that may be achieved after processing by ECAP, HPT or by a combination of the two methods. The use of an

Al-7075 alloy and a ZK60 alloy also provides information on the behavior of both f.c.c. and h.c.p. metals and permits a direct comparison with the earlier single-step data.

2. Experimental materials and procedures

The experiments used a commercial aluminum-based Al-7075 alloy with a composition (in wt%) of 5.6 % Zn, 2.5 % Mg and 1.6 % Cu and a ZK60 magnesium alloy with a composition (in wt%) of 5.5 % Zn and 0.5 % Zr. Both alloys were received as extruded rods with diameters of 10.0 mm and they were sectioned perpendicular to the extrusion direction to give billets with lengths of ~65 mm for ECAP processing. The aluminum alloy was annealed in air at 753 K for 1 h and then cooled to room temperature to give elongated grains with an average diameter of ~8 μm . The magnesium alloy was processed without annealing and with an initial grain size of ~5 μm . Both alloys were processed initially by ECAP and then shortly thereafter by HPT.

The processing by ECAP was performed at 473 K using a hydraulic press with a total capacity of 150 tonnes. The ECAP facility consisted of a solid die having an abrupt internal channel angle, Φ , of 110° and an outer angle denoting the arc of curvature, Ψ , of 20° . The billets were processed by ECAP through 4 passes using route B_C in which the billets are rotated for 90° in the same direction around the extrusion direction after each individual pass [39]. This processing route was selected due to its ability to produce equiaxed UFG microstructures having large fractions of high-angle grain boundaries [40-42]. The strain imposed by ECAP was calculated using the relationship [43]

$$\varepsilon_N = \frac{N_P}{\sqrt{3}} \left[2 \cot \left(\frac{\Phi}{2} + \frac{\Psi}{2} \right) + \Psi \operatorname{cosec} \left(\frac{\Phi}{2} + \frac{\Psi}{2} \right) \right] \quad (2)$$

where ε_N is the total strain imposed after multiple ECAP passes and N_p is the number of passes. According to the geometry and angles of the ECAP facility, a total strain of ~ 0.8 is imposed on the billets after each passage through the die [43]. All billets processed by ECAP were visually inspected to ensure there was no macroscopic damage.

After processing by ECAP, the billets of both alloys were sectioned perpendicular to their extrusion directions into disks having thicknesses of ~ 1.2 - 1.5 mm. These sections were made at a distance of ~ 1 cm away from the ends after processing through 4 passes in order to avoid any internal cracking or damage that may be present. All disks were then polished with abrasive papers to thicknesses of ~ 0.82 mm and processed by HPT at room temperature through total numbers of turns, N , of $1/8$ to 20 turns. A fractional number of turns was used specifically to determine the evolution of hardness during the very early stages of processing following the procedure also used in some earlier studies [36,44-49].

The HPT facility operated under quasi-constrained conditions in which a very small outflow of material occurs around the peripheral region of each disk [50,51]. For processing, samples were placed in a depression at the center of the lower anvil, the anvils were brought together to impose a high pressure and the lower anvil was then rotated giving concurrent torsional straining of the disks. Full details of the HPT processing technique was given earlier [52] except that in this investigation no lubricant was applied to the anvil prior to processing. During HPT the imposed pressure on the aluminum-based samples was 6.0 GPa and on the magnesium samples the pressure was 2.0 GPa. The von Mises equivalent strain, ε , in samples processed by HPT may be calculated from the relationship [53-55]

$$\varepsilon = \frac{2\pi N.r}{h\sqrt{3}} \quad (3)$$

where N , r and h are the total numbers of HPT revolutions, the radius and the thickness of the disk, respectively.

Samples processed by ECAP, HPT and a combination of ECAP + HPT were polished using abrasive papers to achieve mirror-like surfaces for microhardness measurements. Microhardness indentations were made using an FM-1e microhardness instrument equipped with a Vickers indenter using a force of 100 gf and a dwell time of 10 s for each individual indentation. The indentations were made along randomly selected diameters on the surfaces of each disk and each microhardness value was recorded as an average of the microhardness values of four separate indentations uniformly displaced around the selected point. The distance between each indentation was 0.3 μm and this was therefore reduced to 0.15 μm due to the averaging process.

Samples of both alloys in the as-received condition, after processing only by HPT and after processing by a combination of ECAP + HPT were polished with 9, 6, 3 and 1 μm diamond suspension and then with a Vibromet vibratory polisher using 0.04 μm colloidal silica. Microstructural analysis was performed on these samples using an analytical field emission scanning electron microscope (SEM) JEOL JSM-7001F equipped with an electron back-scattered diffraction (EBSD) detector. The operating voltage in the EBSD analysis was 15 kV for the aluminium alloy and 7 kV for the magnesium alloy. The EBSD patterns were collected at a working distance of 15 mm with a sample tilt of 70°. A step size of 0.05 – 0.1 μm was used in

the microstructural images and orientation imaging microscopy (OIMTM) was used to record the microstructural data. A clean-up procedure was performed in the OIM analyzer and this included grain dilation (GD) and grain confidence index (CI) standardizations. Datum points with $CI < 0.1$ were eliminated from the images. In all images, misorientation differences between neighboring grains of more than 15° were defined as high-angle grain boundaries (HAGB) and those between $2^\circ - 15^\circ$ were defined as low-angle grain boundaries (LAGB). The misorientation angles were measured using grain-to-grain misorientations rather than pixel-to-pixel misorientations to avoid having an apparent excess of low-angle boundaries [56,57].

3. Experimental results

Samples in the as-received condition and processed by ECAP, HPT and ECAP + HPT were tested at room temperature using Vickers microhardness testing and scanning electron microscopy equipped with an EBSD detector. The results are described in the following sections.

3.1 Microhardness measurements

Plots of the hardness evolution against equivalent strain for the Al-7075 alloy and the ZK60 alloy are shown in Fig. 1(a) and (b), respectively, where datum points are recorded for ECAP only, HPT only and a combination of ECAP through 4 passes followed by HPT: the data for HPT only are delineated by a best-fitting solid line, the combination of ECAP and HPT by a dashed line and for ECAP only there are only two points recorded in each plot because of the very low strains imposed in the ECAP procedure by comparison with HPT. These plots demonstrate that the microhardness values of both alloys increase with increasing equivalent strain until they level out and reach saturation microhardness values. It is also apparent that both alloys reach good hardness homogeneity after processing by only HPT and by a combination of

ECAP + HPT. The saturation limit for the Al-7075 alloy after only HPT reaches $H_v \approx 230$ and the limit reaches $H_v \approx 250$ after processing by ECAP through 4 passes followed by HPT. The saturation limits differ in a significant way in the ZK60 alloy as shown in Fig 1 (b) where the saturation decreases from $H_v \approx 125$ after processing only by HPT to $H_v \approx 115$ after processing by a combination of ECAP + HPT.

Figure 2 presents double-logarithmic plots of the microhardness values against the equivalent strain for the Al-7075 and ZK60 alloys processed by HPT in (a) and (c) and by a combination of ECAP + HPT in (b) and (d). The slopes of these plots denote the hardenability exponent, η , as obtained from the relationship

$$H_v = K' \varepsilon_{eq}^{\eta} \quad (4)$$

where H_v is the Vickers microhardness, K' is a material constant and ε_{eq} is the equivalent strain. This relationship is in a different form from the well-known Hollomon equation [58] where stress is replaced by the microhardness values and the strain hardening index is replaced by the hardenability exponent: more details on the derivation of this relationship were given elsewhere [38]. It is apparent from Fig. 2 that for both alloys there are decreases in the values of the hardenability exponents between the samples processed by HPT and those processed by ECAP + HPT. In addition, both alloys reach homogeneity at a higher value of equivalent strain after processing by a combination of ECAP + HPT compared to processing only by HPT.

3.2 Microstructural analysis

Figure 3 shows the OIM images for the Al-7075 alloy in (a) the as-annealed condition, (b) after processing by HPT through 5 turns and (c) after processing by ECAP through 4 passes

(p) + HPT through 20 turns (t). These conditions were chosen due to the advent of homogeneity in the disks because it is apparent from Fig. 2 that there is hardness homogeneity across the disks after processing through these strain values. The unit triangle in Fig. 3 denotes the difference in misorientation angles as represented by the different colors. The high-angle grain boundaries are given by black lines and the low-angle grain boundaries are represented by yellow lines in the microstructural images. The average grain sizes were calculated using the OIM software. It was determined that the Al-7075 sample had elongated grains in the annealed condition with an average size of $\sim 8 \mu\text{m}$ whereas after processing by HPT the microstructure was composed of homogeneous equiaxed grains with an average grain size of $\sim 500 \text{ nm}$. The average grain size was further refined to a value of $\sim 310 \text{ nm}$ after processing by ECAP through 4 passes + HPT through 20 turns.

For comparison, Fig. 4 shows the microstructural evolution in the ZK60 alloy (a) in the initial extruded condition, (b) after processing by HPT through 5 turns and (c) after processing by ECAP through 4 passes and HPT through 10 turns. It is apparent from Fig. 4 that the initial average grain size is $\sim 5 \mu\text{m}$ but this value is reduced to $\sim 700 \text{ nm}$ after processing by HPT through 5 turns and then increases to $\sim 2.2 \mu\text{m}$ after further straining through a combination of ECAP for 4 passes + HPT for 10 turns. Thus, the increase in the average grain size in the ZK60 alloy after the combined two-step processing is fully consistent with the decrease in the level of microhardness homogeneity after a combination of ECAP + HPT as shown in Fig. 1(b).

4. Discussion

4.1 The significance of hardening and softening in SPD processing

Processing by ECAP or HPT generally leads to significant grain refinement and this was achieved in the Al-7075 and ZK60 alloys used in this investigation. In addition, metallic

materials processed by HPT generally exhibit a hardness saturation when the equivalent strain is increased. However, in some limited numbers of materials there may be an initial strain hardening and then a subsequent strain softening. This was first reported in the HPT processing of high purity aluminum [59] but the same effect, termed hardening with recovery, has been observed also in other materials [60]. This leads to the possibility that SPD processing may produce either a strengthening or a weakening effect [61]. For example, significant weakening was reported in several materials including the Zn-Al and Pb-Sn alloys by increasing the equivalent strain in processing by HPT [62-64]. There are also examples of weakening in processing by ECAP as in the Al-7034 alloy where the loss of strength was attributed to the fragmentation of rod-like MgZn_2 precipitates and a partial loss of the hardening metastable η' -phase during ECAP [65].

In the present experiments, the results show a consistent strengthening in the Al-7075 alloy with increasing combinations of SPD processing so that, as anticipated in most metals, the hardness in Fig. 1(a) after a combination of ECAP and HPT is significantly higher than after processing only by HPT. By contrast, the results in the ZK60 alloy are different in Fig. 1(b) because they reveal a marked weakening when the HPT processing is applied after ECAP. There is a direct explanation for this unexpected effect based on a set of comprehensive results reported earlier for the same ZK60 alloy after processing by ECAP [66]. In these earlier experiments, it was shown that transition phase rod-shaped $\text{Mg}_1\text{Zn}_1'$ precipitates are visible in the extruded alloy and these precipitates are especially effective in blocking dislocation motion on the basal planes. However, it was demonstrated that these precipitates tend to fragment in SPD processing by ECAP at 473 K and also they evolve into the equilibrium Mg_1Zn_1 phase where both of these changes effectively reduce the overall strength of the alloy. In practice, it is reasonable to

anticipate that this same trend will be enhanced in the present experiments due to the much higher hydrostatic stresses imposed during processing by HPT at room temperature and this will lead to a reduced hardening after a combination of processing by ECAP and HPT as recorded directly in Fig. 1(b). Thus, the ZK60 alloy, unlike the Al-7075 alloy and most other metals, becomes weaker during this combination of different processing procedures.

4.2 The significance of the minimum grain size attained in combinations of SPD processing

A model was developed recently to give the minimum grain size in materials processed by HPT [33]. According to this model, the minimum grain size from HPT processing is dependent upon the processing conditions including the processing temperature and on physical parameters including the stacking fault energy and activation energy.

Based on the results obtained in the present investigation, it is readily apparent that the minimum grain size obtained in a material, and consequently the level of hardness saturation, is specifically dependent upon the initial microstructure of the processed material. The minimum grain size attainable in the aluminum Al-7075 alloy after processing only by HPT is ~500 nm but this value is reduced to ~310 nm after processing by ECAP through 4 passes followed by HPT. However, the opposite trend is observed in the magnesium ZK60 alloy where the minimum grain size increases from ~700 nm after processing only by HPT through 5 turns to ~2.2 μm after processing by a combination of ECAP + HPT. This unusual result is due to the precipitate fragmentation occurring as a consequence of the very high imposed hydrostatic stresses in HPT processing and the result establishes unambiguously that the minimum grain size attained in any material is specifically dependent upon the processing condition imposed prior to HPT. It is concluded, therefore, that there is no specific grain size that can be reasonably documented as a minimum grain size applicable to the HPT processing of any selected alloy.

5. Summary and conclusions

1. The saturation hardness achieved at high strains in HPT processing is dependent upon the microstructural conditions within the material prior to processing.
2. The saturation hardness values after processing by a combination of ECAP + HPT are higher for Al-7075 and lower for ZK60 than those achieved after processing only by HPT. The increase in hardness in Al-7075 is due to the increasing grain refinement with additional processing and the decrease in hardness in ZK60 is due to precipitation fragmentation and changes in the phases during processing under high hydrostatic pressures.
3. Samples of both materials exhibit less hardenability after processing by a combination of ECAP + HPT compared to processing only by HPT.
4. Consistent with the hardness data, the average grain size in Al-7075 was reduced from ~500 nm after HPT to ~310 nm after ECAP + HPT and in ZK60 the grain size changed from ~700 nm after processing by HPT to ~2.2 μm after processing by ECAP + HPT.

Acknowledgement

This work was supported by the National Science Foundation of the United States under Grant No. DMR-1160966.

References

- [1] R.Z. Valiev, R.K. Islamgaliev, I.V. Alexandrov, Bulk nanostructured materials from severe plastic deformation, *Prog. Mater. Sci.* 45 (2000) 103-189
- [2] R.Z. Valiev, Y. Estrin, Z. Horita, T.G. Langdon, M.J. Zehetbauer, Y.T. Zhu, Producing bulk ultrafine-grained materials by severe plastic deformation, *JOM* 58(4) (2006) 33-39.
- [3] T.G. Langdon, Twenty-five years of ultrafine-grained materials: Achieving exceptional properties through grain refinement, *Acta Mater.* 61 (2013) 7035-7059.
- [4] R.Z. Valiev, T.G. Langdon, Principles of equal-channel angular pressing as a processing tool for grain refinement, *Prog. Mater. Sci.* 51 (2006) 881-981.
- [5] A.P. Zhilyaev, T.G. Langdon, Using high-pressure torsion for metal processing: Fundamentals and applications, *Prog. Mater. Sci.* 53 (2008) 893-979.
- [6] K. Matsubara, Y. Miyahara, Z. Horita, T.G. Langdon, Developing superplasticity through a combination of extrusion and ECAP, *Acta Mater.* 51 (2003) 3073-3084
- [7] J. Xu, M. Shirooyeh, J. Wongsan-Ngam, D. Shan, B. Guo, T.G. Langdon, Hardness homogeneity and micro-tensile behavior in a magnesium AZ31 alloy processed by equal-channel angular pressing, *Mater. Sci. Eng. A* 586 (2013) 108-114
- [8] X. Zhao, X. Yang, X. Liu, C.T. Wang, Y. Huang, T.G. Langdon, Processing of commercial purity titanium by ECAP using a 90 degrees die at room temperature, *Mater. Sci. Eng. A* 607 (2014) 482-489
- [9] Y. Han, J. Li, G. Huang, Y. Lv, X. Shao, W. Lu, D. Zhang, Effect of ECAP numbers on microstructure and properties of titanium matrix composite, *Mater. Des.* 75 (2015) 113-119
- [10] M. Alawadhi, S. Sabbaghianrad, Y. Huang, T.G. Langdon, Direct influence of recovery behavior on mechanical properties in oxygen-free copper processed using different SPD techniques: HPT and ECAP, *J. Mater. Res. Tech.* (2017) in press, <http://dx.doi.org/10.1016/j.jmrt.2017.05.005>
- [11] A.P. Zhilyaev, B.K. Kim, G.V. Nurislamova, M.D. Baró, J.A. Szpunar, T.G. Langdon, Orientation imaging microscopy of ultrafine-grained nickel, *Scripta Mater.* 46 (2002) 575-580
- [12] A.P. Zhilyaev, G.V. Nurislamova, B.K. Kim, M.D. Baró, J.A. Szpunar, T.G. Langdon, Experimental parameters influencing grain refinement and microstructural evolution during high-pressure torsion, *Acta Mater.* 51 (2003) 753-765
- [13] J. Wongsan-Ngam, M. Kawasaki, T.G. Langdon, Achieving homogeneity in a Cu-Zr alloy processed by high-pressure torsion, *J. Mater. Sci.* 47 (2012) 7782-7788

- [14] A.P. Zhilyaev, K. Oh-ishi, T.G. Langdon, T.R. McNelley, Microstructural evolution in commercial purity aluminum during high-pressure torsion, *Mater. Sci. Eng. A* 410-411 (2005) 277-280
- [15] Z. Horita, T.G. Langdon, Microstructures and microhardness of an aluminum alloy and pure copper after processing by high-pressure torsion, *Mater. Sci. Eng. A* 410-411 (2005) 422-425
- [16] K. Edalati, A. Yamamoto, Z. Horita, T. Ishihara, High-pressure torsion of pure magnesium: Evolution of mechanical properties, microstructures and hydrogen storage capacity with equivalent strain, *Scripta Mater.* 64 (2011) 880-883
- [17] C. Yang, M. Song, Y. Liu, S. Ni, S. Sabbaghianrad, T.G. Langdon, Evidence for a transition in deformation mechanism in nanocrystalline pure titanium processed by high-pressure torsion, *Phil. Mag.* 96 (2016) 1632-1642
- [18] S. Sabbaghianrad, T.G. Langdon, Developing superplasticity in an aluminum matrix composite processed by high-pressure torsion, *Mater. Sci. Eng. A* 655 (2016) 36-43
- [19] Hall EO, The deformation and ageing of mild steel: III discussion of results, *Proc. Phys. Soc. B* 64 (1951) 747-753
- [20] Petch NJ, Cleavage strength of polycrystals, *J. Iron Steel Inst.* 174 (1953) 25-28
- [21] Y.S. Sato, Y. Kurihara, S.H.C. Park, H. Kokawa, N. Tsuji, Friction stir welding of ultrafine grained Al alloy 1100 produced by accumulative roll-bonding, *Scripta Mater.* 50 (2004) 57-60
- [22] V.V. Stolyarov, Y.T. Zhu, T.C. Lowe, R.K. Islamgaliev, R.Z. Valiev, A two step SPD processing of ultrafine-grained titanium, *Nanostruct. Mater.* 11 (1999) 947-954
- [23] A.P. Zhilyaev, G.V. Nurislamova, S. Suriñach, M.D. Baró, T.G. Langdon, Calorimetric measurements of grain growth in ultrafine-grained nickel, *Mater. Phys. Mech.* 5 (2002) 23-30
- [24] A.P. Zhilyaev, J. Gubicza, S. Suriñach, M.D. Baró, T.G. Langdon, Calorimetric and X-ray measurements in ultrafine-grained nickel, *Mater. Sci. Forum* 426-432 (2003) 4507-4512
- [25] A.P. Zhilyaev, B.K. Kim, J.A. Szpunar, M.D. Baró, T.G. Langdon, The microstructural characteristics of ultrafine-grained nickel, *Mater. Sci. Eng. A* 391 (2005) 377-389
- [26] V.V. Popov, E.N. Popova, A.V. Stolbovskiy, Nanostructuring Nb by various techniques of severe plastic deformation, *Mater. Sci. Eng. A* 539 (2012) 22-29
- [27] J. Wongsan-Ngam, H. Wen, T.G. Langdon, Microstructural evolution in a Cu-Zr alloy processed by a combination of ECAP and HPT, *Mater. Sci. Eng.* 579 (2013) 126-135

- [28] S. Sabbaghianrad, J. Wongsan-Ngam, M. Kawasaki, T.G. Langdon, An examination of the saturation microstructures achieved in ultrafine-grained metals processed by high-pressure torsion, *J. Mater. Res. Tech.* 3 (2014) 319-326
- [29] S. Sabbaghianrad, T.G. Langdon, An evaluation of the saturation hardness in an ultrafine-grained aluminum 7075 alloy processed using different techniques, *J. Mater. Sci.* 50 (2015) 4357-4365
- [30] A.P. Zhilyaev, J. Gubicza, G. Nurislamova, Á. Révész, S. Suriñach, M.D. Baró, T. Ungár, Microstructural characterization of ultrafine-grained nickel, *Phys. Stat. Sol.* 198 (2003) 263-271
- [31] F.A. Mohamed, A dislocation model for the minimum grain size obtainable by ball milling, *Acta Mater.* 51 (2003) 4107-4119
- [32] F.A. Mohamed, S.S. Dheda, On the minimum grain size obtainable by equal channel angular pressing, *Mater. Sci. Eng.* A580 (2013) 227-230
- [33] F.A. Mohamed, S.S. Dheda, On the minimum grain size obtainable by high-pressure torsion, *Mater. Sci. Eng.* A558 (2012) 59-63
- [34] R. Pippan, S. Scheriau, A. Taylor, M. Hafok, A. Hohenwarter, A. Bachmaier, Saturation of fragmentation during severe plastic deformation, *Annu. Rev. Mater. Res.* 40 (2010) 319-343
- [35] R.B. Figueiredo, T.G. Langdon, Grain refinement and mechanical behaviour of a magnesium alloy processed by ECAP, *J. Mater. Sci.* 45 (2010) 4827-4836
- [36] S. Sabbaghianrad, M. Kawasaki, T.G. Langdon, Microstructural evolution and the mechanical properties of an aluminum alloy processed by high-pressure torsion, *J. Mater. Sci.* 47 (2012) 7789-7795
- [37] S.A. Torbati-Sarraf, T.G. Langdon, Mechanical properties of ZK60 magnesium alloy processed by high-pressure torsion, *Adv. Mater. Res.* 922 (2014) 767-772
- [38] S.A. Torbati-Sarraf, S. Sabbaghianrad, R.B. Figueiredo, T.G. Langdon, Orientation imaging microscopy and microhardness in a ZK60 magnesium alloy processed by high-pressure torsion, *J. All. Comp.* 712 (2017) 185-193
- [39] M. Furukawa, Y. Iwahashi, Z. Horita, M. Nemoto, T.G. Langdon, The shearing characteristics associated with equal-channel angular pressing, *Mater. Sci. Eng.* A257 (1998) 328-332
- [40] K. Oh-ishi, Z. Horita, M. Furukawa, M. Nemoto, T.G. Langdon, Optimizing the rotation conditions for grain refinement in equal-channel angular pressing, *Metall. Mater. Trans. A* 29A (1998) 2011-2013

- [41] C. Xu, M. Furukawa, Z. Horita, T.G. Langdon, The evolution of homogeneity and grain refinement during equal-channel angular pressing: A model for grain refinement in ECAP, *Mater. Sci. Eng. A* 398 (2005) 66-76
- [42] T.G. Langdon, The principles of grain refinement in equal-channel angular pressing, *Mater. Sci. Eng. A* 462 (2007) 3-11
- [43] Y. Iwahashi, J. Wang, Z. Horita, M. Nemoto, T.G. Langdon, Principles of equal-channel angular pressing for the processing of ultrafine-grained materials, *Scripta Mater.* 35 (1996) 143-146
- [44] C. Xu, Z. Horita, T.G. Langdon, Microstructural evolution in pure aluminum in the early stages of processing by high-pressure torsion, *Mater. Trans.* 51 (2010) 2-7.
- [45] A.Y. Khereddine, F.H. Larbi, M. Kawasaki, T. Baudin, D. Bradai, T.G. Langdon, An examination of microstructural evolution in a Cu-Ni-Si alloy processed by HPT and ECAP, *Mater. Sci. Eng. A* 576 (2013) 149-155
- [46] J. Wongsan-Ngam, T.G. Langdon, Microstructural evolution and grain refinement in a Cu-Zr alloy processed by high-pressure torsion, *Mater. Sci. Forum* 783-786 (2014) 2635-2640
- [47] S.A. Torbati-Sarraf, S. Sabbaghianrad, T.G. Langdon, Microstructural properties, thermal stability and superplasticity of a ZK60 Mg alloy processed by high-pressure torsion, *Letters Mater.* 53 (2015) 287-293
- [48] S. Sabbaghianrad, T.G. Langdon, Mechanical properties and microstructural behavior of a metal matrix composite processed by severe plastic deformation techniques, *MRS Adv.* 1 (2016) 3865-3870
- [49] R.B. Figueiredo, S. Sabbaghianrad, A. Giwa, J.R. Greer, T.G. Langdon, Evidence for exceptional low temperature ductility in polycrystalline magnesium processed by severe plastic deformation, *Acta Mater.* 122 (2017) 322-331
- [50] R.B. Figueiredo, P.R. Cetlin, T.G. Langdon, Using finite element modeling to examine the flow processes in quasi-constrained high-pressure torsion, *Mater. Sci. Eng. A* 528 (2011) 8198-8204
- [51] R.B. Figueiredo, P.H.R. Pereira, M.T.P. Aguilar, P.R. Cetlin, T.G. Langdon, Using finite element modeling to examine the temperature distribution in quasi-constrained high-pressure torsion, *Acta Mater.* 60 (2012) 3190-3198.
- [52] M. Kawasaki, T.G. Langdon, The significance of strain reversals during processing by high-pressure torsion, *Mater. Sci. Eng. A* 498 (2008) 341-348
- [53] R.Z. Valiev, Y.V. Ivanisenko, E.F. Rauch, B. Baudelet, Structure and deformation behavior of Armco iron subjected to severe plastic deformation, *Acta Mater.* 44 (1996) 4705-4712

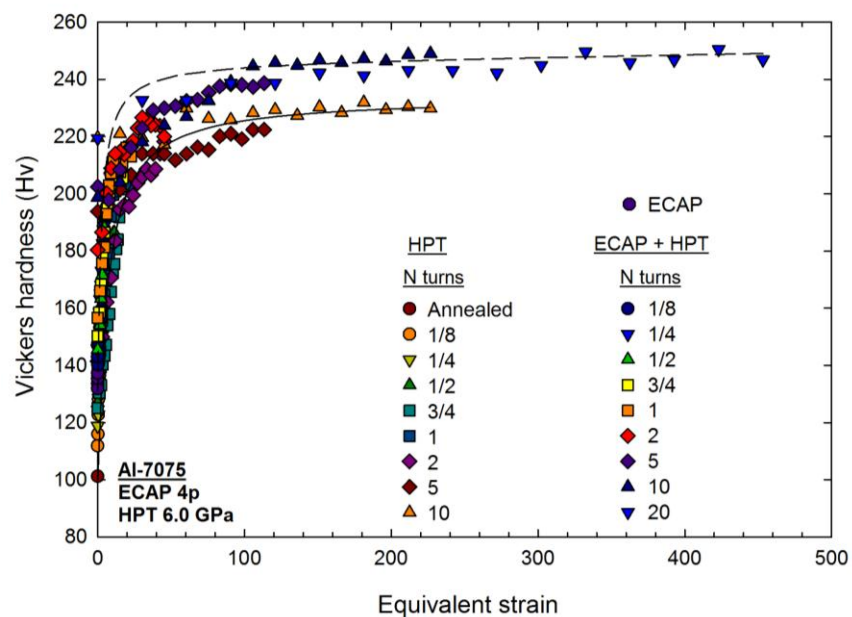
- [54] F. Wetscher, A. Vorhauer, R. Stock, R. Pippan, Structural refinement of low alloyed steels during severe plastic deformation, *Mater. Sci. Eng. A* 387-389 (2004) 809-816
- [55] F. Wetscher, R. Pippan, S. Sturm, F. Kauffmann, C. Scheu, G. Dehm, TEM investigations of the structural evolution in a pearlitic steel deformed by high-pressure torsion, *Metall. Mater. Trans. A* 37A (2006) 1963-1968
- [56] L.S. Toth, B. Beausir, C.F. Gu, Y. Estrin, N. Scheerbaum, C.H.J. Davies, Effect of grain refinement by severe plastic deformation on the next-neighbor misorientation distribution, *Acta Mater.* 58 (2010) 6706-6716
- [57] L.S. Toth, C. Gu, Ultrafine-grain metals by severe plastic deformation, *Mater. Charact.* 92 (2014) 1-14
- [58] J.H. Hollomon, A method to determine the stress-strain relationship of BCC materials, *Trans. Metall. Soc. AIME* 162 (1945) 268-274
- [59] C. Xu, Z. Horita, T.G. Langdon, The evolution of homogeneity in processing by high-pressure torsion, *Acta Mater.* 55 (2007) 203-212
- [60] M. Kawasaki, Different models of hardness evolution in ultrafine-grained materials processed by high-pressure torsion, *J. Mater. Sci.* 49 (2014) 18-34
- [61] T.G. Langdon, Strengthening and weakening in the processing of ultrafine-grained metals, *Kovove Mater.* 53 (2015) 213-219
- [62] B.B. Straumal, B. Baretzky, A.A. Mazilkin, F. Phillipp, O.A. Kogtgenkova, M.N. Volkov, R.Z. Valiev, Formation of nanograined structure and decomposition of supersaturated solid solution during high pressure torsion of Al-Zn and Al-Mg alloys, *Acta Mater.* 52 (2004) 4469-4478
- [63] N.X. Zhang, M. Kawasaki, Y. Huang, T.G. Langdon, Microstructural evolution in two-phase alloys processed by high-pressure torsion, *J. Mater. Sci.* 48 (2013) 4582-4591
- [64] M. Kawasaki, H.J. Lee, B. Ahn, A.P. Zhilyaev, T.G. Langdon, Evolution of hardness in ultrafine-grained metals processed by high-pressure torsion, *J. Mater. Res. Tech.* 3 (2014) 311-318
- [65] C. Xu, M. Furukawa, Z. Horita, T.G. Langdon, Influence of ECAP on precipitate distributions in a spray-cast aluminum alloy, *Acta Mater.* 53 (2005) 749-758
- [66] B. Li, S. Joshi, K. Azevedo, E. Ma, K.T. Ramesh, R.B. Figueiredo, T.G. Langdon, Dynamic testing at high strain rates of an ultrafine-grained magnesium alloy processed by ECAP, *Mater. Sci. Eng. A* 517 (2009) 24-29

Fig. 1 Vickers microhardness values plotted against equivalent strain for (a) Al-7075 aluminum alloy and (b) ZK60 magnesium alloy after processing by HPT (solid line) or by a combination of ECAP + HPT (dashed line): the results for Al-7075 are consistent with expectations but the results for ZK60 are different.

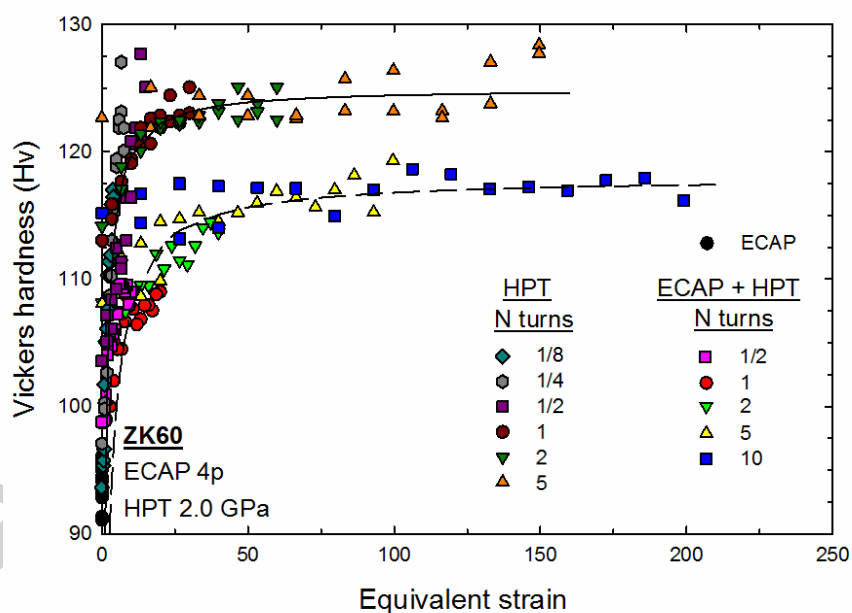
Fig. 2 A double-logarithmic plot of Vickers microhardness values against equivalent strain for Al-7075 after processing by (a) HPT and (b) ECAP + HPT and for ZK60 after processing by (c) HPT and (d) ECAP + HPT: the slopes of the lines give the hardenability exponents.

Fig. 3 Microstructural images for the Al-7075 alloy (a) in the as-annealed condition and after processing by (b) HPT through 5 turns and (c) ECAP for 4 passes + HPT through 20 turns: the unit triangle denotes the misorientations.

Fig. 4 Microstructural images for the ZK60 alloy (a) in the initial extruded condition and after processing by (b) HPT through 5 turns and (c) ECAP for 4 passes + HPT through 20 turns: the unit triangle denotes the misorientations.



(a)



(b)

Fig. 1 Vickers microhardness values plotted against equivalent strain for (a) Al-7075 aluminum alloy and (b) ZK60 magnesium alloy after processing by HPT (solid line) or by a combination of ECAP + HPT (dashed line): the results for Al-7075 are consistent with expectations but the results for ZK60 are different.

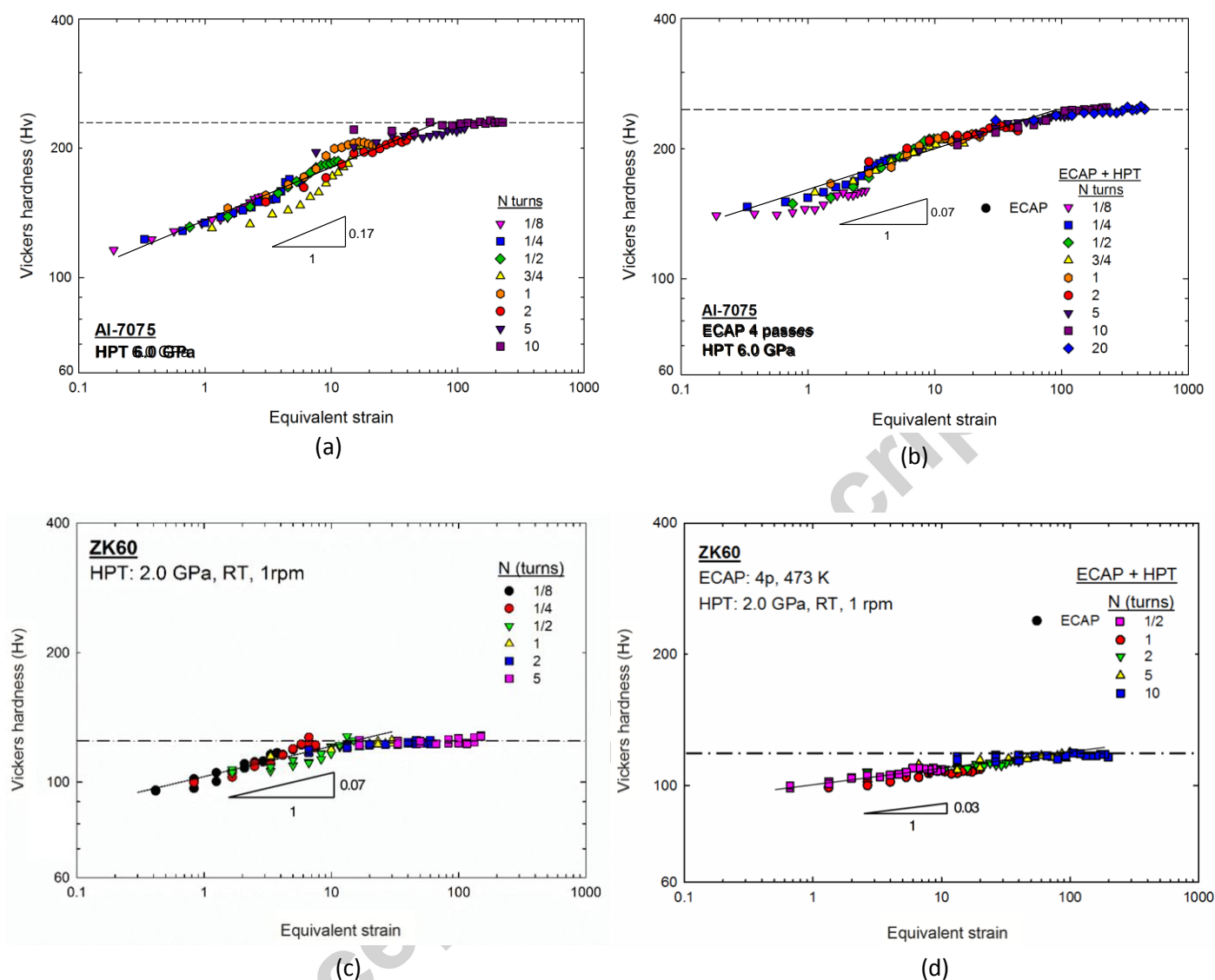


Fig. 2 A double-logarithmic plot of Vickers microhardness values against equivalent strain for Al-7075 after processing by (a) HPT and (b) ECAP + HPT and for ZK60 after processing by (c) HPT and (d) ECAP + HPT: the slopes of the lines give the hardenability exponents

Al-7075

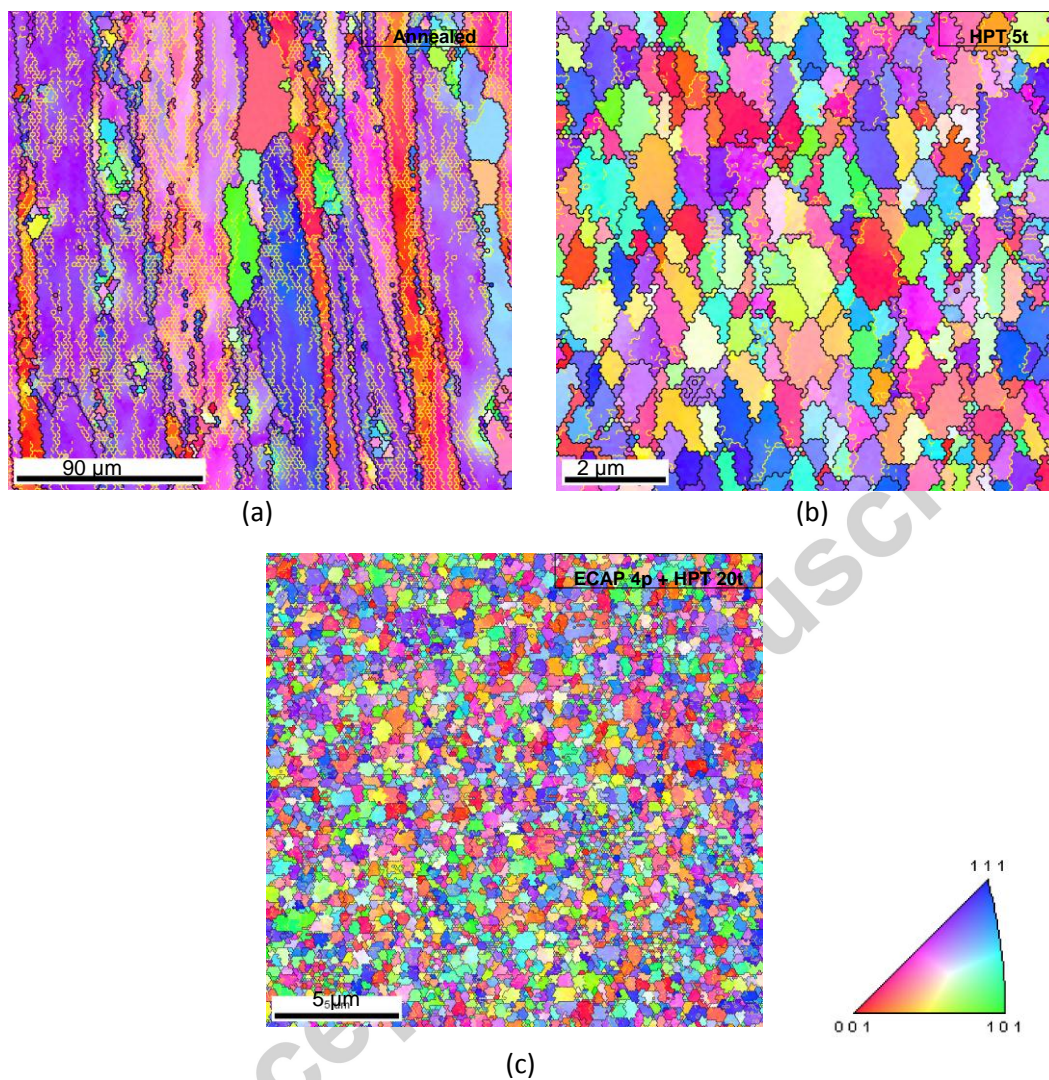


Fig. 3 Microstructural images for the Al-7075 alloy (a) in the as-annealed condition and after processing by (b) HPT through 5 turns and (c) ECAP for 4 passes + HPT through 20 turns

ZK60

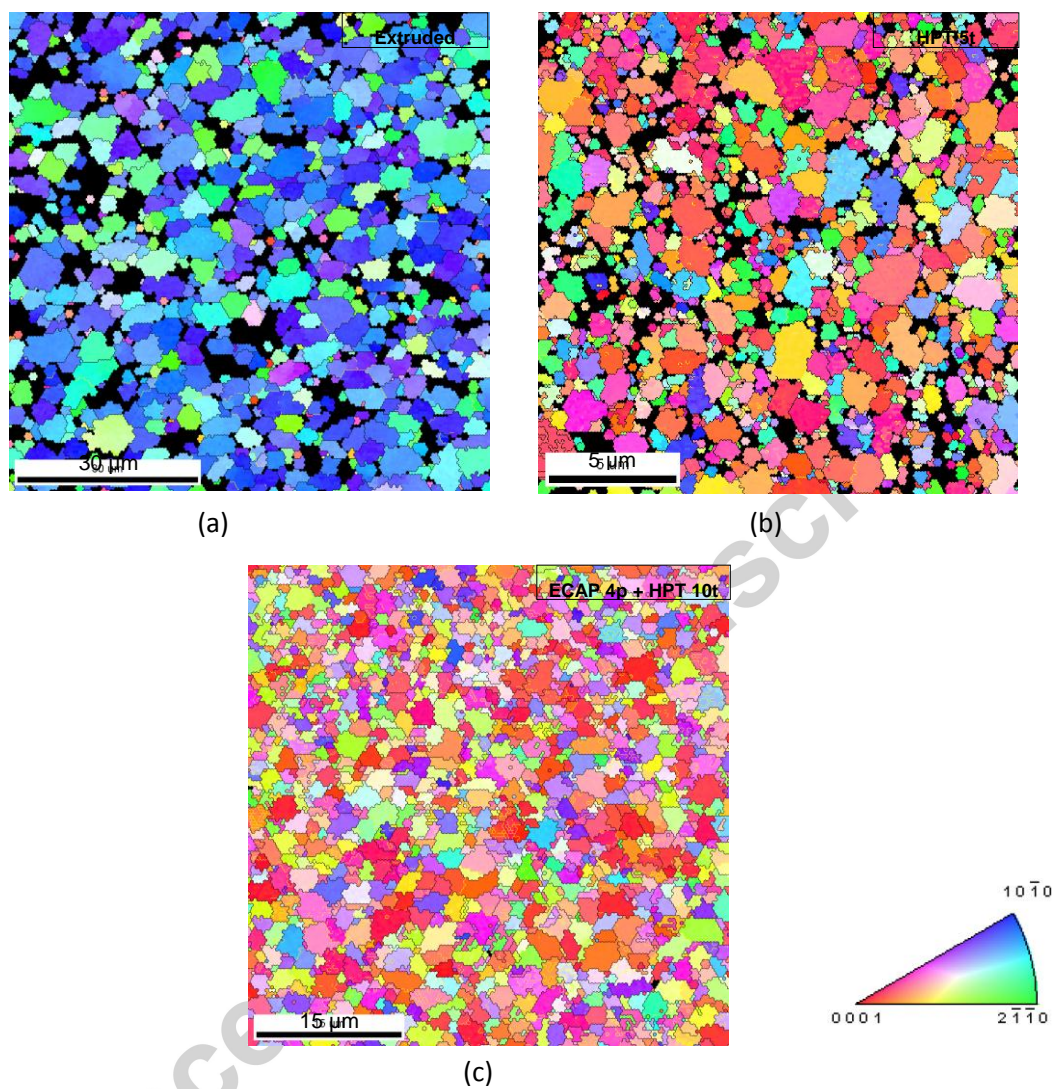


Fig. 4 Microstructural images for the ZK60 alloy (a) in the initial extruded condition and after processing by (b) HPT through 5 turns and (c) ECAP for 4 passes + HPT through 20 turns: the unit triangle denotes the misorientations.